NONRELATIVISTIC ELECTRONICS

INTERACTION BETWEEN A TUBULAR BEAM OF CHARGED PARTICLES AND AN ANISOTROPIC DISPERSIVE SOLID-STATE CYLINDER

Yu.O. Averkov[1,2], Yu.V. Prokopenko[1,3], and V.M. Yakovenko[1]
[1]A.Ya. Usikov Institute for Radiophysics and Electronics of National Academy of Sciences of Ukraine, Kharkov, Ukraine;
[2]V.N. Karazin Kharkiv National University, Kharkov, Ukraine;
[3]Kharkiv National University of Radioelectronics, Kharkov, Ukraine
E-mail: yuriyaverkov@gmail.com; prokopen@ire.kharkov.ua; yavm@ire.kharkov.ua

The interaction between a tubular beam of charged particles and a nonmagnetic anisotropic dispersive medium of cylindrical configuration has been investigated. It has been found the absolute instability of bulk-surface waves that occurs because of peculiarities of the anisotropic cylinder properties. The resonance behavior of the permittivity frequency dependence causes the emergence of the sections of dispersion curves of the *E*-type bulk-surface eigenmodes with negative group velocity. It has been shown there are the *E*-type surface eigenmodes and pseudo surface eigenmodes of *E*- and *H*-types in the cylinder.

PACS: 03.50.-z, 52.40.-w, 52.59.-f, 85.45.-w

INTRODUCTION

Investigation of the generation mechanisms of electromagnetic waves that are excited when charged particles move in various electrodynamic systems is important in microwave electronics. To create sources of electromagnetic radiation in the millimeter and submillimeter ranges, the beam instabilities occurring in electrodynamic systems of various kinds are of great interest. Currently, special attention is given to multiwave Cherenkov sources of surface waves [1, 2] and autooscillatory systems based on dielectric resonators [3 - 5], and dielectric Cherenkov masers [6]. Besides, the beam instabilities that occur in electrodynamic systems containing dispersive media are of special interest. In particular, the instabilities of the tubular electron beam that interacts with a plasmalike medium and a left-handed dispersive medium of cylindrical configuration were studied in [7] and [8], respectively.

In the present paper, the interaction between a tubular beam of charged particles and eigenmodes of nonmagnetic cylindrical solid-state waveguide, in which the components of permittivity tensor have frequency dispersion, is theoretically investigated. This crystal-like medium of the waveguide may have the permittivities with the different signs in perpendicular and parallel directions to the optical axis in a certain frequency range. Our goal is to determine the conditions for the excitation of eigenmodes with anomalous dispersion. It will be shown that the interaction of an electron beam with the waveguide eigenmodes gives rise to the absolute instability of the bulk-surface electromagnetic waves, which are the propagating waves in the waveguide and, at the same time, are evanescently confined along the normal to the lateral cylinder surface in vacuum. This means that the anisotropic dispersive media can be used as the delaying structures with "natural feedback" for generation of electromagnetic waves in backward-wave tubes. Besides, the possibility of excitation of weakly damped whispering gallery waves in an anisotropic cylinder [9] will allow the generation of electromagnetic waves in the submillimeter region of the spectrum.

1. STATEMENT OF THE PROBLEM AND BASIC EQUATIONS

Consider a nonmagnetic cylindrical solid-state waveguide with the radius ρ_0 occupying the region $0 \le \rho \le \rho_0$, $0 \le \varphi \le 2\pi$, and $-\infty \le z \le +\infty$ (Fig. 1). The cylinder is made of an anisotropic single crystal, the optical axis of which orientates parallel to the symmetry axis Z of cylinder. A tubular electron beam with the radial thickness a and density $N_0(\rho)$ moves in vacuum at a distance of ρ_b from the cylinder axis at a velocity v_0. We assume that the charges of electrons are compensated by the background of positive charges and the thickness of the beam a is much smaller than the other spatial scales of the electrodynamic system under consideration. Hence, the undisturbed beam density can be represented as $N_0(\rho) = N_0 a\delta(\rho - \rho_b)$, where N_0 is the equilibrium beam density and $\delta(\rho - \rho_b)$ is the Dirac delta function.

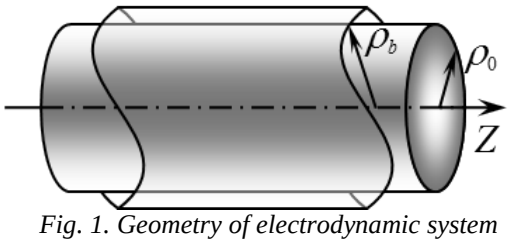

Fig. 1. Geometry of electrodynamic system

In case of linear approximation, the disturbed beam current density at a point with the radius-vector $\mathbf{r}$ at a moment t has the form

$$\mathbf{j}(\mathbf{r},t) = eN_0(\rho)\mathbf{v}(\mathbf{r},t) + e\mathbf{v}_0 N(\mathbf{r},t),$$

where e is the electron charge, and $N(\mathbf{r},t)$ and $\mathbf{v}(\mathbf{r},t)$ are the variable components of the beam density and the electron velocity, respectively. Hereafter, we will suppose that the radial component of the beam current density is equal to zero because of the chosen model of the electron beam.

System of equations, which describes the interaction between the electron beam and the cylinder eigenmodes, represents the Maxwell equations supplemented with the linearized continuity and motion equations for the beam electrons:

$$\mathrm{rot}\mathbf{H}(\mathbf{r},t)=\frac{1}{c}\frac{\partial}{\partial t}\mathbf{D}(\mathbf{r},t)+\frac{4\pi}{c}\mathbf{j}(\mathbf{r},t)\,, \quad (1)$$

$$\mathrm{rot}\mathbf{E}(\mathbf{r},t)=-\frac{1}{c}\frac{\partial}{\partial t}\mathbf{H}(\mathbf{r},t)\,, \quad (2)$$

$$\mathrm{div}\,\mathbf{D}(\mathbf{r},t)=4\pi eN(\mathbf{r},t)\,, \quad (3)$$

$$\mathrm{div}\,\mathbf{H}(\mathbf{r},t)=0\,, \quad (4)$$

$$e\frac{\partial N(\mathbf{r},t)}{\partial t}+\mathrm{div}\mathbf{j}(\mathbf{r},t)=0\,,$$

$$\frac{\partial \mathbf{v}(\mathbf{r},t)}{\partial t}+v_0\frac{\partial \mathbf{v}(\mathbf{r},t)}{\partial z}=\frac{e}{m}\left(\mathbf{E}(\mathbf{r},t)+\frac{1}{c}[\mathbf{v}_0,\mathbf{H}(\mathbf{r},t)]\right),$$

where m is the electron mass, c is the velocity of light in vacuum, $\mathbf{E}(\mathbf{r},t)$ and $\mathbf{H}(\mathbf{r},t)$ are the electric and magnetic field vectors, and $\mathbf{D}(\mathbf{r},t)$ is the electric displacement vector that is related with the $\mathbf{E}(\mathbf{r},t)$ -vector by the constitutive equations

$$D_i(\mathbf{r},t)=\int_{-\infty}^{t}\hat{\varepsilon}_{ij}(t-t')E_j(\mathbf{r},t')dt'\,,$$

where $\hat{\varepsilon}_{ij}(t-t')$ is the influence function that characterizes the efficiency of the field action in time. Indices i and j correspond to one of the directions along the coordinate axes ρ, φ, and z. Here, the summation by the index j is carried out with a search of all directions. In vacuum we have $\hat{\varepsilon}_{ij}(t-t')=\delta_{ij}\delta(t-t')$, where δ_{ij} is the Kronecker symbol. Note that the difference nature of the kernels of the integrals is due to the homogeneity of the waveguide properties in time.

In order to derive the dispersion equation for the electromagnetic waves in the electrodynamic system under consideration, it is necessary to satisfy certain boundary conditions at $\rho=\rho_0$ and $\rho=\rho_b$. These conditions are as follows. First, the tangential components of the electric and magnetic fields are continuous at $\rho=\rho_0$. Second, at $\rho=\rho_b$ the tangential components of the magnetic field have to be discontinuous because of the beam current, whereas the tangential components of the electric field are continuous. Note that the normal component of the magnetic field vector remains continuous, whereas the normal component of the electric displacement vector suffers discontinuity because of the disturbed beam charge.

We determine the discontinuities of the tangential components of the magnetic field and the normal component of the electric displacement [in vacuum $D_\rho(\mathbf{r},t)\equiv E_\rho(\mathbf{r},t)$] by integrating (1) and (3) over the infinitesimally small beam thickness. As a result, we have

$$H_\varphi(\mathbf{r},t)\big|_{\rho=\rho_b+0}-H_\varphi(\mathbf{r},t)\big|_{\rho=\rho_b-0}=\frac{4\pi}{c\rho_b}\lim_{\Delta\rho\to 0}\int_{\rho_b-\Delta\rho}^{\rho_b+\Delta\rho}j_z(\mathbf{r},t)\rho d\rho\,,$$

$$H_z(\mathbf{r},t)\big|_{\rho=\rho_b+0}-H_z(\mathbf{r},t)\big|_{\rho=\rho_b-0}=-\frac{4\pi}{c}\lim_{\Delta\rho\to 0}\int_{\rho_b-\Delta\rho}^{\rho_b+\Delta\rho}j_\phi(\mathbf{r},t)d\rho\,,$$

$$E_\rho(\mathbf{r},t)\big|_{\rho=\rho_b+0}-E_\rho(\mathbf{r},t)\big|_{\rho=\rho_b-0}=\frac{4\pi e}{\rho_b}\lim_{\Delta\rho\to 0}\int_{\rho_b-\Delta\rho}^{\rho_b+\Delta\rho}N(\mathbf{r},t)\rho d\rho\,.$$

We represent all variables in the form of the set of space-time harmonics, for instance:

$$\mathbf{E}(\mathbf{r},t)=\sum_{n=-\infty}^{\infty}\int_{-\infty}^{\infty}\int_{-\infty}^{\infty}\mathbf{E}_n(\rho,q_z,\omega)\exp[i(q_z z+n\varphi-\omega t)]dq_z d\omega\,, \quad (5)$$

where ω, q_z, and n are the frequency, longitudinal wave number, and the number of the spatial harmonic (coinciding with the azimuthal mode index), respectively; $i^2=-1$. Then we have

$$D_i(\rho,q_z,\omega)=\varepsilon_{ij}(\omega)E_j(\rho,q_z,\omega)\,,$$

where $\varepsilon_{ij}(\omega)=\int_0^\infty\varepsilon_{ij}(\tau)\exp(i\omega\tau)d\tau$ is the permittivity tensor of medium.

Consider the medium inside the cylinder, which consists of anisotropic oscillators characterized by a set of eigenfrequencies ω_L, ω_r, and ω_s. Such a medium corresponds to a crystal, whose permittivity tensor has a diagonal form with components $\varepsilon_\perp$ and $\varepsilon_\parallel$, where the indices "$\perp$" and "$\parallel$" indicate the material properties in the perpendicular and parallel directions to the optical axis of the crystal, respectively. We assume that the frequency dependences $\varepsilon_\perp(\omega)$ and $\varepsilon_\parallel(\omega)$ have the form [10 - 13]

$$\varepsilon_\perp(\omega)=\varepsilon_0-\frac{\omega_L^2}{\omega^2-\omega_r^2}\,,\ \varepsilon_\parallel(\omega)=\varepsilon_0-\frac{\omega_L^2}{\omega^2-\omega_s^2}\,,$$

where ε_0 is the background value of the dielectric constant of the crystal determined as the high-frequency limit of $\varepsilon_\perp(\omega)$ and $\varepsilon_\parallel(\omega)$. It is clear that there are such frequency bands in which $\varepsilon_\perp(\omega)$ and $\varepsilon_\parallel(\omega)$ have negative values.

In particular, these dependences $\varepsilon_\perp(\omega)$ and $\varepsilon_\parallel(\omega)$ characterize the magnetized collisionless semiconductor medium, in which

$$\varepsilon_\perp(\omega)=\varepsilon_0+\sum_{\alpha=1}^{2}\frac{\omega_{L\alpha}^2}{\omega_{r\alpha}^2}\,;\ \varepsilon_\parallel(\omega)=\varepsilon_0-\sum_{\alpha=1}^{2}\frac{\omega_{L\alpha}^2}{\omega^2}\,,$$

where $\omega_{L\alpha}^2=4\pi e_\alpha^2 n_\alpha/m_\alpha$ and $\omega_{r\alpha}=e_\alpha H_0/m_\alpha c$, e_α, m_α and n_α are the charge, mass and the majority-carrier concentration of the α -kind: electrons (α = 1) and holes (α = 2), respectively, H_0 is the induction of an external magnetic field (whose vector orientates parallel to the symmetry axis Z of cylinder). At the same time $\omega_s=0$ and $\omega_r\equiv\omega_{r\alpha}$, and $\omega_{r\alpha}>>\omega$ because of $H_0\to\infty$.

If we take into account (5), we can rewrite the original equations (1) - (4) for the axial spectral components of the field in the region inside the cylindrical solid-state waveguide ($\rho\le\rho_0$) in the following form:

$$\left[\frac{1}{\rho}\frac{\partial}{\partial\rho}\rho\frac{\partial}{\partial\rho}+\left(q_E^2-\frac{n^2}{\rho^2}\right)\right]E_{zn}(\rho,q_z,\omega)=0\,, \quad (6a)$$

$$\left[\frac{1}{\rho}\frac{\partial}{\partial\rho}\rho\frac{\partial}{\partial\rho}+\left(q_H^2-\frac{n^2}{\rho^2}\right)\right]H_{zn}(\rho,q_z,\omega)=0\,, \quad (6b)$$

where $q_H^2=\varepsilon_\perp\omega^2/c^2-q_z^2$ and $q_E^2=q_H^2\varepsilon_\parallel/\varepsilon_\perp$ are the square of the transverse (radial) wave number of electromagnetic wave of *H*- and *E*-types, respectively. The corresponding equations for the axial spectral components of the field in vacuum ($\rho>\rho_0$) outside the electron beam ($\rho\neq\rho_b$) are

$$\left[\frac{1}{\rho}\frac{\partial}{\partial\rho}\rho\frac{\partial}{\partial\rho}+\left(q^2-\frac{n^2}{\rho^2}\right)\right]\begin{Bmatrix}E_{zn}(\rho,q_z,\omega)\\H_{zn}(\rho,q_z,\omega)\end{Bmatrix}=0\,, \quad (6c)$$

where $q^2=\omega^2/c^2-q_z^2$. If $q_H^2,q_E^2,q^2>0$, the equations (6) have the form of the Bessel equations, whereas if $q_H^2,q_E^2,q^2<0$ they are the modified Bessel equations.

We are only interested in the waves, which have surface behavior in vacuum. For these waves the condition $q^2<0$ is satisfied. Exactly, these waves are excited by the beam of charged particles provided the Cherenkov resonance $\omega=q_zv_0$ [14]. Indeed, for the nonrelativistic electron velocities ($\beta\ll1$, where $\beta=v_0/c$ is the dimensionless electron velocity) considered herein, we have $\omega^2/c^2\ll q_z^2$ and $q^2<0$. Taking into account the aforesaid, we represent the expressions for the spectral components of the electromagnetic field $E_{zn}(\rho,q_z,\omega)$ and $H_{zn}(\rho,q_z,\omega)$ in the following form:

$$E_{zn}(\rho,q_z,\omega)=\begin{cases}\begin{cases}A_n^E J_n(q_E\rho), & q_E^2>0\\ A_n^E I_n(|\,q_E\,|\,\rho), & q_E^2<0\end{cases}, & \rho\le\rho_0\\ B_n^E K_n(|\,q\,|\,\rho)+C_n^E I_n(|\,q\,|\,\rho), & \rho_0<\rho<\rho_b,\\ D_n^E K_n(|\,q\,|\,\rho), & \rho>\rho_b,\end{cases}$$

$$H_{zn}(\rho,q_z,\omega)=\begin{cases}\begin{cases}A_n^H J_n(q_H\rho), & q_H^2>0\\ A_n^H I_n(|\,q_H\,|\,\rho), & q_H^2<0\end{cases}, & \rho\le\rho_0\\ B_n^H K_n(|\,q\,|\,\rho)+C_n^H I_n(|\,q\,|\,\rho), & \rho_0<\rho<\rho_b,\\ D_n^H K_n(|\,q\,|\,\rho), & \rho>\rho_b,\end{cases}$$

where $J_n(u)$ is the nth order Bessel function of the first kind; $I_n(u)$ and $K_n(u)$ are the modified functions of the first kind (Infeld function) and the second kind (Macdonald function), respectively; $A_n^{E,H}$, $B_n^{E,H}$, $C_n^{E,H}$, and $D_n^{E,H}$ are the arbitrary constants. The choice of the solution is due to the fulfillment of finiteness conditions for $E_{zn}(\rho,q_z,\omega)$ and $H_{zn}(\rho,q_z,\omega)$ at $\rho\to0$ and $\rho\to\infty$. At $\varepsilon_\perp\beta^2>1$ the radial distribution of the field component $H_{zn}(\rho,q_z,\omega)$ inside the cylinder is described by Bessel functions $J_n(q_H\rho)$, and at $\varepsilon_\perp\beta^2<1$ it is described by modified Bessel functions $I_n(|\,q_H\,|\,\rho)$. Using the Maxwell equations, we express transverse spectral components of the electromagnetic fields in the cylinder region ($\rho<\rho_0$), as well as in the annular gap ($\rho_0<\rho<\rho_b$), and on the other side of the beam ($\rho>\rho_0$) via the components $E_{zn}(\rho,q_z,\omega)$ and $H_{zn}(\rho,q_z,\omega)$.

We note that in the nonrelativistic case, if $\beta^2\ll1$, but $\varepsilon_\perp\beta^2>1$, the discontinuities of the tangential magnetic field components $H_{\varphi n}(\rho,q_z,\omega)$ and $H_{zn}(\rho,q_z,\omega)$ at the beam surface ($\rho=\rho_b$) are small values of the order of $O(\beta)$. Therefore, in what follows, in the boundary conditions at the beam surface ($\rho=\rho_b$), we suppose these components are continuous, and take into account only the discontinuity of the normal (radial) electric field component $E_{\rho n}(\rho,q_z,\omega)$.

Assuming the beam is nonrelativistic, and satisfying the above-mentioned boundary conditions at the cylinder and electron beam surfaces, we obtain the following dispersion equation for the beam-cylinder coupled waves:

$$\Delta_n[(\omega-q_zv_0)^2-\Gamma(q_z,n)\omega_b^2]=\alpha\omega_b^2\,, \quad (7)$$

where $\omega_b=\sqrt{4\pi e^2N_0/m}$ is the plasma frequency of beam electrons, $\Gamma(q_z,n)$ is the depression factor of space-charge forces [15], found to be

$$\Gamma(q_z,n)=(n^2+q_z^2\rho_b^2)I_n(|\,q_z\,|\,\rho_b)K_n(|\,q_z\,|\,\rho_b)\times$$
$$\times\frac{a}{\rho_b}\left[1-\frac{I_n(|\,q_z\,|\,\rho_0)K_n(|\,q_z\,|\,\rho_b)}{I_n(|\,q_z\,|\,\rho_b)K_n(|\,q_z\,|\,\rho_0)}\right].$$

The value α is the coupling factor of the beam with cylinder eigenmodes that has the form

$$\alpha=\frac{a}{\rho_b}(n^2+q_z^2\rho_b^2)\frac{K_n^2(|\,q_z\,|\,\rho_b)}{q_z^2\rho_0^2K_n^2(|\,q_z\,|\,\rho_0)}\Delta_n^H\,,$$

$$\Delta_n=a_n^2-\Delta_n^H\Delta_n^E\,,\ a_n^2=\left[\frac{nq_z\omega(\varepsilon_\perp-1)}{q^2q_H^2\rho_0^2c}\right]^2,$$

$$\Delta_n^E=\frac{1}{|\,q\,|\,\rho_0}\frac{K_n'(|\,q\,|\,\rho_0)}{K_n(|\,q\,|\,\rho_0)}+\frac{\varepsilon_\parallel}{q_E\rho_0}\frac{J_n'(q_E\rho_0)}{J_n(q_E\rho_0)}\,,$$

$$\Delta_n^H=\frac{1}{|\,q\,|\,\rho_0}\frac{K_n'(|\,q\,|\,\rho_0)}{K_n(|\,q\,|\,\rho_0)}+\frac{1}{q_H\rho_0}\frac{J_n'(q_H\rho_0)}{J_n(q_H\rho_0)}\,.$$

The primed cylindrical functions denote their derivatives with respect to the argument. Note that equation (7) has the form analogous to the characteristic equation of a traveling-wave tube [15]. In our case, it describes the interaction of the beam space-charge waves (SCWs) with the cylinder eigenmodes. Dispersion equations for the beam SCWs and the cylinder eigenmodes are described by the following equations:

$$(\omega-q_zv_0)^2-\Gamma(q_z,n)\omega_b^2=0\,,\ \text{and}\ \Delta_n=0\,.$$

The solutions of the equation $\Delta_n=0$ determine the eigenfrequencies $\omega_{ns}=\omega_{ns}'-i\omega_{ns}''$, $\omega_{ns}''\ge0$, of the cylindrical waveguide with the hybrid *E*- and *H*-type waves. The azimuthal mode index n = 0, 1, 2, 3, … corresponds to half the number of field variations in the angle φ. The radial index s represents the number of field variations along the radial coordinate ρ and corresponds to the pair of roots order number of the equation $\Delta_n=0$, whose solutions determine the frequencies ω_{ns} of the cylinder eigenmodes with the longitudinal wave

number q_z. In the case of azimuthally-homogeneous symmetric ($n = 0$) waves and axially-homogeneous ($q_z = 0$) oscillations, the indices s correspond to the root order numbers of the homogeneous dispersion equations $\Delta_n^H = 0$ and $\Delta_n^E = 0$, on which the equation $\Delta_n = 0$ splits. In the dispersion equation $\Delta_n = 0$ the value a_n plays the role of the coupling constant between the *E*- and *H*-waves.

The dispersion dependences $\omega_{0s}(q_z)$ of the symmetric eigenmodes H_{0s} and E_{0s} of a solid-state cylinder are determined by the solutions of the dispersion equations $\Delta_0^H = 0$ and $\Delta_0^E = 0$, respectively. The solutions of the equation $\Delta_n = 0$ at $n \neq 0$ determine the dispersion dependences $\omega_{ns}(q_z)$ of the hybrid EH_{ns} (*H*-type) or HE_{ns} (*E*-type) eigenmodes of the waveguide. A unique correspondence of these equation solutions to a specified type of wave (*H*- or *E*-type) can be identified only after determining the dominant longitudinal field component, in other words after comparing the maximum values of the moduli $|H_{zn}(\rho, q_z, \omega_{ns})|$ and $|E_{zn}(\rho, q_z, \omega_{ns})|$ [9]. In the case of HE_{ns} mode the constant A_n^H is determined through the constant A_n^E, and vice versa, in the case of EH_{ns} mode the constant A_n^E is determined through the constant A_n^H.

The quantities contained in equation (7) correspond to the cylinder eigenmodes with transverse wave numbers for which the conditions $q_H^2 > 0$ and $q_E^2 > 0$ are satisfied. In the case of $q_H^2 < 0$ and $q_E^2 < 0$, the terms $J_n'(q_H\rho_0)/q_H\rho_0 J_n(q_H\rho_0)$ and $\varepsilon_\parallel J_n'(q_E\rho_0)/q_E\rho_0 J_n(q_E\rho_0)$ in Δ_n^H and Δ_n^E in the equation (7) acquire the form $-I_n'(|q_H|\rho_0)/|q_H|\rho_0 I_n(|q_H|\rho_0)$ and $-\varepsilon_\parallel I_n'(|q_E|\rho_0)/|q_E|\rho_0 I_n(|q_E|\rho_0)$, respectively.

Depending on the signs of q_H^2 and q_E^2, the eigenmodes of the waveguide have different types (Table). In Table, the type classification of eigenmodes is given in accordance with the terminology in [16 - 18].

Types of eigenmodes of a solid-state cylinder located in vacuum

The sign of the square of the transverse wave number		The sign of the permittivity		Type of eigenmodes	Reference
q_H^2	q_E^2	$\varepsilon_\perp(\omega)$	$\varepsilon_\parallel(\omega)$		
+	+	+	+	bulk-surface	[16]
+	–	+	–	surface and/or bulk-surface symmetric, pseudo-surface hybrid	[16 - 18]
–	+	+	–	bulk-surface	[16]
–	+	–	+	bulk-surface	[16]
–	–	–	–	surface	[17, 18]
–	–	+	+	do not exist (forbidden zone)	

We note that the pseudo-surface axial-homogeneous ($q_z = 0$) eigenmodes and pseudo-surface azimuthally homogeneous symmetric ($n = 0$) eigenmodes do not exist because they are hybrid. The absence of cylinder eigenmodes is determined by the absence of solutions of the dispersion equation $\Delta_n = 0$. In this case, the corresponding frequency and wavenumber regions form forbidden zones in the spectra of the waveguide waves.

When the cylinder is absent in the electrodynamic system, i.e. in the case of $\rho_0 \to 0$, we have $\alpha/\Delta_n \to 0$, and the solutions of the dispersion equation (7) determine the frequencies of the slow (ω_-) and fast (ω_+) beam SCWs: $\omega_- = q_z v_0 - R_0(q_z, n)\omega_b$ and $\omega_+ = q_z v_0 + R_0(q_z, n)\omega_b$, where $R_0(q_z, n) = \sqrt{\Gamma_0(q_z, n)}$ is the reduction factor [15], and

$$\Gamma_0(q_z, n) = \lim_{\rho_0 \to 0} \Gamma(q_z, n) =$$

$$= \frac{a}{\rho_b}(n^2 + q_z^2\rho_b^2) I_n(|q_z|\rho_b) K_n(|q_z|\rho_b).$$

Consequently, the phase velocities of the slow (ω_-/q_z) and fast (ω_+/q_z) SCWs are less and greater than the beam velocity v_0, respectively.

When the beam electrons move along the lateral surface of a cylindrical solid-state waveguide ($\rho_b = \rho_0$) or close to it ($\rho_b \neq \rho_0$) under the condition that the reduced plasma frequency of the beam $R(q_z, n)\omega_b << |\delta\omega|$, where $R(q_z, n) = \sqrt{\Gamma(q_z, n)}$ and $\delta\omega$ are small additions to the frequencies ω_{ns} that arise due to interaction between the beam and cylinder eigenmodes, the Cherenkov effect, under which $\omega_{ns} = q_z v_0$, is realized in an electrodynamic system [8]. The instability increments of the beam-cylinder coupled waves are expressed as follows [8]:

$$\operatorname{Im}\delta\omega = \frac{\sqrt{3}}{2}\left|\frac{\alpha(\omega_{ns})}{\Delta'_{n\omega}(\omega_{ns})}\right|^{1/3} \omega_b^{2/3}, \qquad (8)$$

where $\alpha(\omega_{ns})$ is the coupling factor α at the resonance frequency ω_{ns}. We note that $\operatorname{Im}\delta\omega \propto N_0^{1/3}$. Consequently, the excitation of the cylinder eigenmodes by resonance beam particles (whose velocity satisfies the condition $\omega_{ns} = q_z v_0$) is coherent [19].

If the electron beam is transported at a considerable distance from the cylindrical surface of the waveguide ($\rho_b > \rho_0$), the anomalous Doppler effect is realized in the system. In this case, the resonance interaction of the beam with the cylinder eigenmodes is realized at frequencies $\omega_{ns}^{\pm} = \omega_\pm = q_z v_0 \pm R(q_z, n)\omega_b$ [8]. The instability arises only in the interaction of slow space-charge waves with the cylinder eigenmodes. The instability increments are determined as follows [8]

$$\mathrm{Im}\,\delta\omega = \left[\frac{\alpha(\omega_{ns}^{-})\omega_b}{2R(q_z,n)\Delta'_{n\omega}(\omega_{ns}^{-})}\right]^{1/2}. \qquad (9)$$

It follows that $\mathrm{Im}\,\delta\omega \propto N_0^{1/4}$.

For a fundamental understanding of the interaction mechanism between the charged particles of a tubular beam and cylinder eigenmodes, below we present the results of numerical analysis of the dispersion equation (7), and the expressions for the instability increments (8) and (9).

2. NUMERICAL ANALYSIS OF THE DISPERSION EQUATION

The dispersion equation $\Delta_n = 0$ has dimensionless form, which emphasizes its universality. The dimensionless form of the waveguide eigenfrequencies is provided by their normalization to the characteristic frequency $\omega_0 = c/\rho_0$, taking into account the identity of the cylindrical waveguide configuration.

We suppose that the cylindrical solid-state waveguide under study has the characteristic frequency $\omega_0 = 6\cdot10^{10}$ s^{-1}, which corresponds to the radius $\rho_0 = 0.5$ cm, and is made of an artificial material with following parameters: $\varepsilon_0 = 2$, $\omega_L/\omega_0 = 3.5$, $\omega_r/\omega_0 = 4$, $\omega_s/\omega_0 = 6$. The values of the equilibrium beam electron density N_0, the radial thickness of the beam a, and the directed motion velocity of the beam electrons are chosen as follows: $N_0 = 7.6\cdot10^{10}$ cm^{-3}, and a =0.05 cm, and $v_0 = 0.3c$, respectively. For the selected system parameters, we have $\omega_b^2/\omega_0^2 \approx 0.07$. The normalized frequencies $\omega_\parallel/\omega_0$ and $\omega_\perp/\omega_0$, at which $\varepsilon_\parallel(\omega) = 0$ and $\varepsilon_\perp(\omega) = 0$, have values 6.49 and 4.7, respectively.

2.1. SPECTRA OF THE CYLINDER EIGENMODES

Fig. 2 shows the spectra of the cylinder symmetric ($n = 0$) and the unsymmetrical ($n \neq 0$) eigenmodes.

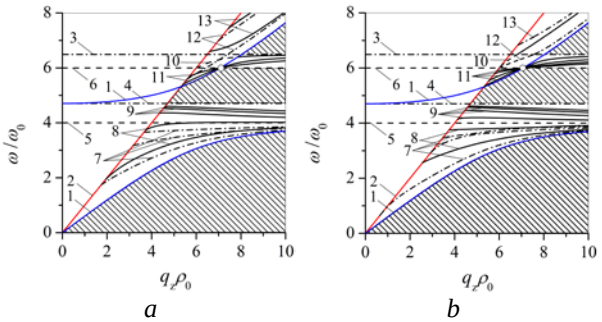

Fig. 2. Dispersion dependences of the symmetric (a) and the hybrid (b) eigenmodes of the cylinder

Lines 1 correspond to the frequencies and the longitudinal wave numbers at which the transverse wave numbers q_H vanish. Line 2 refers to the light line in vacuum $\omega/\omega_0 = q_z\rho_0$ when $q = 0$. We are only interested in the ranges of frequencies and longitudinal wavenumbers of the waveguide eigenmodes where the condition $q^2 < 0$ is satisfied. Lines 3 and 4 correspond to the frequencies $\omega_\parallel/\omega_0$ and $\omega_\perp/\omega_0$. Lines 5 and 6 are for the normalized eigenfrequencies of the oscillators of artificial material in perpendicular (ω_r/ω_0) and parallel (ω_s/ω_0) directions to the symmetry axis of the cylinder, respectively. Lines 7 and 8 represent the spectra of the *H*- and *E*-type bulk-surface waves, for which $q_E^2 > 0$ and $q_H^2 > 0$, namely, the symmetric modes $H_{0\,1}$, $E_{0\,1}$, $H_{0\,2}$, $H_{0\,3}$ and $E_{0\,2}$ (Fig. 2,a), and the hybrid modes $EH_{1\,1}$, $HE_{1\,1}$, $EH_{1\,2}$, $EH_{1\,3}$ and $HE_{1\,2}$ (Fig. 2,b) that are arranged in ascending order of frequencies ω_{ns}. Note that the density of the dispersion curves of the *H*-type eigenmodes increases with radial index s in the frequency range $0 < \omega < \omega_r$ at $\omega_{ns} \to \omega_r - 0$ (from below). In doing so, the wave number q_H, which enters into the argument of the Bessel function $J_0(q_H\rho_0)$ in the dispersion equation $\Delta_0^H = 0$, changes from $q_H = 0$ at $\omega = 0$ and $q_z = 0$ to $q_H \to \infty$ at $\omega = \omega_r$. The number of the E-type eigenmodes remains finite in the same frequency range. This is because the transverse wave number q_E, which enters into the argument of the Bessel function $J_0(q_E\rho_0)$ in the dispersion equation $\Delta_0^E = 0$, changes from $q_E = 0$ at $\omega = 0$ and $q_z = 0$ to $q_E = \omega_r\sqrt{\varepsilon_\parallel(\omega_r)}/c$ at $\omega = \omega_r$. Curves 9 correspond to the dispersion dependences of the bulk-surface symmetric E_{0s} (see Fig. 2,a) and the hybrid HE_{1s} (see Fig. 2,b) modes with $s = 3, 4, 5, 6$ in the frequency range $\omega_r < \omega < \omega_\perp$. The density of the dispersion curves of the waveguide eigenmodes increases with radial index s when their frequencies ω_{ns} tend to the frequency $\omega_\perp$ from below ($\omega_{ns} \to \omega_\perp - 0$). In the frequency range $\omega_s < \omega < \omega_\parallel$ the dashed parts of the dispersion branches 10 correspond to the surface symmetric *E*-type waves in Fig. 2,a and the pseudo-surface hybrid $HE_{1\,1}$ waves in Fig. 2,b for which $q_E^2 < 0$, $q_H^2 > 0$ and $\varepsilon_\parallel(\omega) < 0$, $\varepsilon_\perp(\omega) > 0$. In Fig. 2,a, the branch of the surface waves (curve 10) intersects the curve $q_H = 0$ (curve 1) and converts to the branch of the bulk-surface $E_{0\,1}$ waves for which $q_E^2 > 0$. Note that the dispersion equation $\Delta_n^E = 0$ has no solutions at the very point of intersection. In Fig. 2,b the branch of the pseudo-surface hybrid $HE_{1\,1}$ wave converts continuously to the branch of the bulk-surface $HE_{1\,1}$ wave at $\omega > \omega_\parallel$. Lines 11 represent the spectra of the bulk-surface symmetric E_{0s} (see Fig. 2,a) and the hybrid HE_{1s} (see Fig. 2,b) modes. The $E_{0\,1}$ and the $HE_{1\,1}$ modes have the lowest frequencies in the frequency range $\omega_\perp < \omega < \omega_s$, whereas the $E_{0\,2}$ and the $HE_{1\,1}$ modes have the highest frequencies in the frequency range $\omega_s < \omega < \omega_\parallel$. In the frequency range $\omega_\perp < \omega < \omega_s$ the density of the dispersion curves of the waveguide eigenmodes increases with radial index s at $\omega_{ns} \to \omega_s - 0$ when $\varepsilon_\parallel(\omega) \to +\infty$, whereas in the frequency range $\omega_s < \omega < \omega_\parallel$ the density of the corre-

sponding curves increases with radial index s at $\omega_{ns} \to \omega_s + 0$ when $\varepsilon_{\|}(\omega) \to -\infty$. The dispersion curves go from one frequency band to another through the zero forbidden zone (the point of intersection of the branches and the curve $q_H = 0$ in Fig. 2) [20]. Under the transition of the branches of the symmetric modes between frequency bands, the radial indices are increased by one in the direction of increasing frequencies ω_{0s}. The series of curves 12 in Fig. 2,a show the spectra of the bulk-surface symmetric eigenmodes H_{0s} with s = 1, 2, and they are arranged in order of increasing frequencies ω_{0s}. In Fig. 2,b the dispersion branch 12 refers to the pseudo-surface waves (dashed line) in the frequency range $\omega_s < \omega < \omega_{\|}$, whereas at frequencies $\omega > \omega_{\|}$ it is for the bulk-surface hybrid $EH_{1\,1}$ waves (dash-and-dot line). Note that the conversion of the pseudosurface waves into the bulk-surface ones at the frequency $\omega_{\|}$, when $\varepsilon_{\|} = 0$, accompanies the above mentioned continuous transition of the dispersion branch from one frequency range to another. Lines 13 are the dispersion curves of the bulk-surface symmetric E_{0s} waves (s = 1, 2 in order of increasing frequencies ω_{0s}) in Fig. 2,a and the hybrid $EH_{1\,2}$ waves in Fig. 2,b.

As seen from Fig. 2, the *E*-type bulk-surface waves (curves 9) in the frequency range $\omega_r < \omega < \omega_{\perp}$ have negative group velocities and their dispersion dependences approach asymptotically the straight line $\omega / \omega_0 = \omega_r / \omega_0 + 0$ at $q_z \rho_0 \to \infty$. It is worthwhile to emphasize that the H_{0s} eigenmodes do not exist in this frequency range because the dispersion equation $\Delta_0^H = 0$ has no solutions there. The frequencies and the longitudinal wave numbers of the symmetric E_{0s} modes are determined by the solutions of the dispersion equation $\Delta_0^E = 0$. Beyond the range $\omega_r < \omega < \omega_{\perp}$, the waveguide eigenmodes possess the positive group velocities. In the frequency range $\omega < \omega_r$ at $q_z \rho_0 \to \infty$ the dispersion curves of the bulk-surface eigenmodes approach asymptotically the straight line $\omega / \omega_0 = \omega_r / \omega_0 - 0$, whereas in the frequency range $\omega_s < \omega < \omega_{\|}$ they approach the straight line $\omega / \omega_0 = \omega_{\|} / \omega_0 - 0$. It is interesting to note that in the frequency range $\omega_s < \omega < \omega_{\|}$ the surface, the pseudosurface, and the bulk-surface waves exist simultaneously at one and the same frequency, but have different wavenumbers.

The shaded areas in Fig. 2 show the regions of frequencies and wave numbers where the eigenmodes do not exist in the waveguides under consideration (so-called, forbidden zones). In these regions the corresponding dispersion equations $\Delta_n = 0$ have no solutions. In addition, the frequency band $\omega_r < \omega < \omega_{\perp}$ is forbidden for the *H*-type waves.

Note that the qualitative behavior of the dispersion dependences of cylinder eigenmodes with $n > 1$ is similar to the dependences for the modes with $n = 1$.

In Fig. 3, the radial distributions of the field components $|E_{zn}(\rho, q_z, \omega)|$ of the bulk-surface symmetric E_{0s} (see Fig. 3,a) and hybrid HE_{1s} (see Fig. 3,b) eigenmodes with the indices s = 1, 3 are shown as an example. The distributions of the field axial components are normalized to their maximum values. Dependences 1 correspond to the $E_{0\,1}$ and $HE_{1\,1}$ waves with frequencies $\omega < \omega_r$ and positive group velocities. Dependences 2 correspond to the $E_{0\,3}$ and $HE_{1\,3}$ waves with frequencies in the range $\omega_r < \omega < \omega_{\perp}$. Note that the radial indices represent the number of the total field variations along the radial coordinate, reading from the symmetry axis of the waveguide.

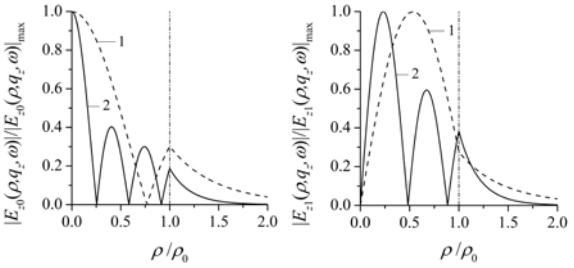

a *b*

Fig. 3. Normalized field distributions of the spectral axial components of the symmetric E_{0s} (a) and hybrid HE_{1s} (b) eigenmodes (s = 1, 3) of the cylindrical waveguide along the radial coordinate

It should be noted that in practice the finite energy losses in the cylinder material cause the predominant existence of the eigenmodes with the radial indices s = 1, 2, 3, whereas the eigenmodes with $s > 3$ are decayed [9, 21]. In fact, a weak decaying of the waveguide eigenmodes is provided by the concentration of their fields near the waveguide cylindrical surface. Such properties are inherent in the modes with azimuthal indices $n >> 1$, for example, in the whispering gallery modes in quasi-optical structures [9].

The fact that the *E*-type bulk-surface eigenmodes of the cylindrical waveguide under consideration possess the negative group velocities in the frequency range $\omega_r < \omega < \omega_{\perp}$ is very important to practical applications because the interaction of these waves with a tubular beam of charged particles results in the absolute instability [7]. It is important to stress that these waves exist in an anisotropic waveguide with permittivities $\varepsilon_{\|} > 0$ and $\varepsilon_{\perp} < 0$ that provides $q_E^2 > 0$ and $q_H^2 < 0$.

2.2. SPECTRA OF COUPLED WAVES: ABSOLUTE AND CONVECTIVE INSTABILITIES

Let us ascertain the nature of the instability that occurs in the Cherenkov resonant interaction between the electron beam and the bulk-surface symmetric eigenmodes of the cylindrical waveguide ($q_z v_0 = \omega_{0s}$) under the conditions $R(q_z, n)\omega_b << |\delta\omega|$ and an extremely small distance of the beam from the cylinder. Henceforward, we suppose that $\rho_b = \rho_0$. To this end, we will use the well-known Sturrock method [8, 19, 22] in the small areas in the vicinities of intersection points of the dispersion dependences of the cylinder eigenmodes with the beam waves $\omega / \omega_0 = \beta q_z \rho_0$ (of the so-called resonance points).

We note that only the *E*-type eigenmodes are unstable because only their fields have a nonzero component of the electric field $E_{z0}(\rho, q_z, \omega)$ with which the nonrelativistic beam electrons interact. All conclusions about the nature of the instabilities remain valid also for the excitation of bulk-surface unsymmetrical modes of the cylindrical waveguide in the small areas in the vicinities of the corresponding resonance points.

Fig. 4 shows the dispersion curves corresponding to the symmetric eigenmodes of the cylindrical waveguide, and to the waves being radiated by the beam electrons, and to the space-charge waves of the beam. Lines 1, 2, 4, 5 and curves 7 - 9 have the same physical meaning as those in Fig. 2. Line 3 is for the beam waves with frequencies $\omega = q_z v_0$. Lines 6 and 10 show the spectra of the slow and the fast space-charge waves of the beam, respectively. Points A and B correspond to the intersections of the dispersion dependence of the beam waves with the dispersion curves of the bulk-surface waves $E_{0\,3}$ and $E_{0\,1}$ in the frequency ranges $\omega_r < \omega < \omega_\perp$ and $0 < \omega < \omega_r$, respectively. The coordinates of these points ($\rho_0 q_{z,res}$, ω_{res}/ω_0) refer to the Cherenkov resonances of the particle-wave type ($q_z v_0 = \omega_{0s}$) [23]. The group velocities of the symmetric electromagnetic waves E_{0s} are determined as follows [8]:

$$v_{gr} = -\left(\frac{\partial \Delta_n^E}{\partial q_z}\right)\left(\frac{\partial \Delta_n^E}{\partial \omega}\right)^{-1}\Bigg|_{\substack{q_z = q_{z,res} \\ \omega = \omega_{res}}},$$

where the partial derivatives $\partial\Delta_n^E/\partial q_z$ and $\partial\Delta_n^E/\partial\omega$ are calculated at the resonance points ($q_{z,res}$, ω_{res}).

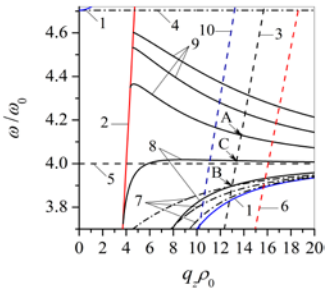

Fig. 4. Dispersion dependences of the cylinder symmetric modes [curves (7)-(9)], and the beam waves (3), and the slow (6) and fast (10) space-charge waves of the beam

In Fig. 4, the intersection points of the dispersion dependence of the slow SCWs (straight line 6) with the dispersion curves of the bulk-surface waves E_{0s} in the frequency range $\omega_r < \omega < \omega_\perp$ (curves 9) are of special interest. These points with coordinates ($\rho_0 q_{z,res}$, ω_{res}/ω_0) refer to the resonances with anomalous Doppler effect of the slow bulk-surface waves with the cylinder symmetric modes ($q_z v_0 - R(q_z, n)\omega_b = \omega_{0s}^-$).

Fig. 5 presents the dispersion dependences of the waves excited by the beam in the small areas in the vicinities of point A with coordinates $\rho_0 q_{z,res} \approx 13.79$, $\omega_{res}/\omega_0 \approx 4.13$ (see Fig. 5,a), and point B with coordinates $\rho_0 q_{z,res} \approx 13.016$, $\omega_{res}/\omega_0 \approx 3.896$ (see Fig. 5,b). These dependences are the solutions of the following equation [8]:

$$(\delta\omega - v_0\delta q_z)^2(\delta\omega - v_{gr}\delta q_z) = \omega_b^2 \frac{a}{\rho_0}\left(\frac{\partial \Delta_n^E}{\partial \omega}\right)^{-1}\Bigg|_{\substack{q_z = q_{z,res} \\ \omega = \omega_{res}}}, \quad (10)$$

where δq_z is the small variation of the corresponding longitudinal wave number $q_{z,res}$. Note that equation (10) is the result of the transformation of equation (7) in the small areas in vicinities of resonance points. Lines 1 and 2 refer to the values $\delta q_z = 0$ and $\delta\omega = 0$, respectively. Line 3 is for the asymptote $\delta\omega/\omega_0 = (v_{gr}/c)\rho_0\delta q_z$, and line 4 is for the beam wave $\delta\omega/\omega_0 = \beta\rho_0\delta q_z$. Curves 5 and 6 are for the bulk-surface modes $E_{0\,3}$ (see Fig. 5,a) and $E_{0\,1}$ (see Fig. 5,b) excited by the beam in the frequency ranges $\omega_r < \omega < \omega_\perp$ and $0 < \omega < \omega_r$, respectively.

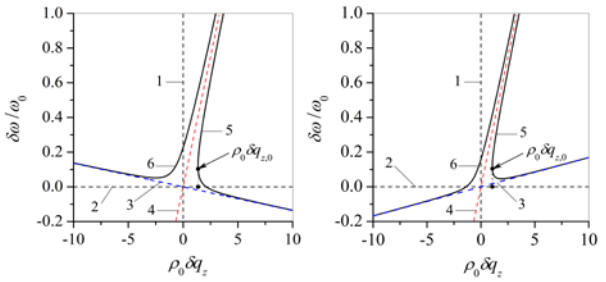

Fig. 5. Dispersion curves of the coupled bulk-surface symmetric waves $E_{0\,3}$ and $E_{0\,1}$ excited by the beam in the small areas in the vicinities of points A (a) and B (b) in Fig. 4, respectively

Since the equation (10) is a cubic one, then, as known, it has three different real roots or one real root and two conjugate complex roots. As one of these complex roots has positive imaginary part, the instability develops. From Fig. 5, it follows that the instabilities occur at values $\rho_0\delta q_z < \rho_0\delta q_{z,0}$ and hold up to values $\rho_0\delta q_z \to -\infty$. It is also clearly seen that that asymptotes 3 and 4 are inclined in different directions in Fig. 5,a and in the same direction in Fig. 5,b with respect to line 2. The negative slope of asymptote 3 in Fig. 5,a and the positive slope of analogous asymptote in Fig. 5,b are caused by the negative and positive values of the group velocities of the $E_{0\,3}$ and $E_{0\,1}$ modes in the frequency ranges $\omega_r < \omega < \omega_\perp$ ($v_{gr}/c \approx -1.35\cdot10^{-2}$) and $0 < \omega < \omega_r$ ($v_{gr}/c \approx 1.7\cdot10^{-2}$), respectively. In accordance with the Sturrock rule [19, 22], this signifies the occurrence of the absolute and convective instabilities in corresponding frequency ranges.

Note that the absolute and convective instabilities are used for the generation and amplification of electromagnetic oscillations, respectively [15, 19, 24, 25].

2.3. ANALYSIS OF INSTABILITY INCREMENTS

Let us dwell on the dependences of instability increments $\mathrm{Im}\,\delta\omega$ for the *E*-type coupled bulk-surface waves on the values of azimuthal *n* and radial *s* mode indices in the frequency range $\omega_r < \omega < \omega_\perp$. These increment values are calculated using formula (8) under the Cherenkov resonance conditions (when $\rho_b = \rho_0$) and the formula (9) under the conditions of the resonance with anomalous Doppler effect (when $\rho_b > \rho_0$).

The values of the absolute instability increments $\mathrm{Im}\,\omega/\omega_0$ of the excited bulk-surface modes E_{0s} and HE_{ns} with azimuthal indices in the range n = 1…20 for the radial indices s = 3, 4, 5 are shown in Fig. 6. Note that the dispersion dependences for the modes with n = 0, 1 (curves 9) are only shown in Figs. 2 and 4. Fig. 6,a shows the increments of the waves excited by the beam under the Cherenkov resonance conditions, when the resonant interaction between the beam electrons and the eigenmodes of the solid-state cylindrical waveguide takes place. Fig. 6,b presents the increments of excited waves under the conditions of the resonance with anomalous Doppler effect, when the interaction between the beam SCWs and the waveguide eigenmodes holds. The increment values are grouped in accordance with the radial index s of cylinder eigenmodes. The dependences of the increment values of the E_{0s} and HE_{ns} modes with the radial indices s = 3, 4, 5 on the azimuthal index n are labeled by the numbers 1, 2, and 3, respectively. As evident from Fig. 6, in the frequency range $\omega_r < \omega < \omega_\perp$ the instability increment values of the *E*-type under the Cherenkov resonance conditions are two orders of magnitude higher than for the Doppler effect. The hybrid modes with three field variations along the radial coordinate (HE_{n3} modes) have the maximum increments. In Fig. 6, the presented dependences have extreme maxima. It is notable that these maxima belong to the coupled hybrid HE_{ns} modes of the whispering gallery [9]. As seen from Fig. 6, as the radial index s increases, the azimuthal index n of the mode with the maximum increment decreases.

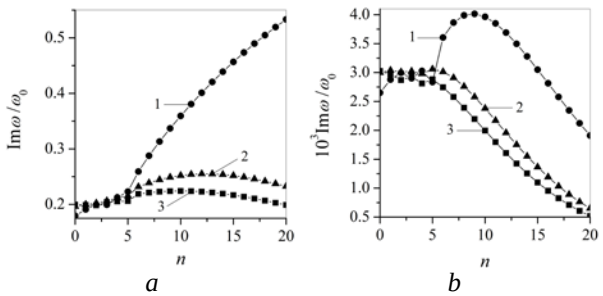

Fig. 6. Increment values of the absolute instability of the coupled bulk-surface waves E_{0s} and HE_{ns} under the Cherenkov resonance conditions (a) and under the conditions of the resonance with anomalous Doppler effect (b)

In Fig. 7, the dependences of the instability increment values of excited E_{03} and HE_{n3} modes on the azimuthal index n are shown for different radial distances between the cylinder and the electron beam $\rho_b - \rho_0$, when the anomalous Doppler effect is realized. The dependences corresponding to the values $\rho_b - \rho_0$ = 0.1, 0.11 and 0.14 cm are labeled by the numbers 1, 2 and 3, respectively. It is seen that the coupled whispering gallery modes, which are excited by a tubular electron beam moving at a minimum distance above the cylinder, possess the greatest values of the increments. The increment values of excited waves decrease with the increase of the distance between the electron beam and the cylinder $\rho_b - \rho_0$. In represent dependences, the HE_{93} mode has the greatest increment. From Fig. 7 it follows that the azimuthal index n of the mode possessed the maximum increment decreases with the increase of $\rho_b - \rho_0$. It is equivalently that the frequency of the most nonstable wave decreases.

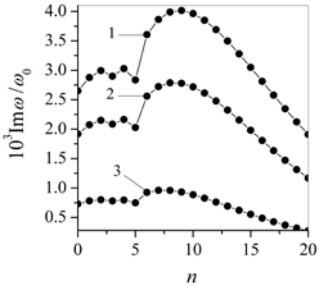

Fig. 7. Instability increment values of the system with the coupled bulk-surface waves E_{03} and HE_{n3} at different distances $\rho_b - \rho_0$ between the cylinder and the electron beam

Thus, the analysis of the absolute instability of the system under consideration suggests that the instability occurs in the frequency range $\omega_r < \omega < \omega_\perp$ where $\varepsilon_\perp(\omega) < 0$ and $\varepsilon_\parallel(\omega) > 0$, and the largest values of the increments correspond to the bulk-surface hybrid whispering gallery modes HE_{n3}.

CONCLUSIONS

The instability of a nonrelativistic tubular electron beam that moves in vacuum above an anisotropic solid-state cylinder has been theoretically examined. It has been assumed that an electron beam is infinitely thin in the radial direction and the components of the cylinder permittivity tensor possess the frequency dispersion. The dispersion equations for eigenmodes of the cylinder and for the coupled modes of the system have been derived. The analysis of the eigenmode properties and the classification of the eigenmodes have been performed. The spectra of the cylinder symmetric and unsymmetrical eigenmodes have been determined. It has been revealed that the bulk-surface waves of the E-type have negative group velocities over a certain frequency range. It has been shown that the existence of such waves is caused by the anisotropic properties of the waveguide with the components of the permittivity $\varepsilon_\perp < 0$ and $\varepsilon_\parallel > 0$, which provide fulfillment of the conditions $q_H^2 < 0$ and $q_E^2 > 0$ in a unique fashion. The existence of the E-type surface symmetric waves and the pseudo-surface hybrid waves of the E- and the H-types in the cylindrical solid-state waveguide has been shown. It has been found that there are frequency ranges where the surface waves, the bulk-surface waves and the pseudo-surface hybrid waves can exist at one and the same frequency, but with different wave numbers. The ranges of both the frequencies and the wave numbers where the eigenmodes in the waveguide under study cannot exist have been specified (so-called forbidden zones). The increments of the instabilities caused by both the Cherenkov and the Doppler effects have been analyzed. It has been demonstrated by the Sturrock rules that the absolute and convective instabilities of the E-type bulk-surface waves occur in different frequency ranges. The numerical analysis of the dependences of

the instability increments of the system under consideration with the symmetric and the bulk-surface hybrid waves of the E-type on the values of azimuthal and radial mode indices for different distances between the electron beam and the cylinder has been performed. It has been established that the coupled bulk-surface whispering gallery HE_{n3} modes excited by the beam have the largest values of the increments.

Thus, the use of the anisotropic dispersive material with the permittivity components $\varepsilon_{\perp}(\omega) < 0$ and $\varepsilon_{\parallel}(\omega) > 0$ as the delaying medium makes possible the generation of the bulk-surface waves over a certain frequency range and eliminates the need for creating artificial feedbacks in slow-wave structures.

REFERENCES

1. N.S. Ginzburg, V.Y. Zaslavskii, A.M. Malkin, and A.S. Sergeev. Relativistic surface-wave oscillators with 1D and 2D periodic structures // *Technical Physics.* 2012, v. 57, iss. 12, p. 1692-1705.
2. N.S. Ginzburg, V.Y. Zaslavskii, A.M. Malkin, and A.S. Sergeev. Quasi-optical theory of coaxial and cylindrical relativistic surface-wave oscillators // *Technical Physics.* 2013, v. 58, iss. 2, p. 267-276.
3. A.V. Dormidontov, A.Ya. Kirichenko, Yu.F. Lonin, A.G. Ponomarev, Yu.V. Prokopenko, G.V. Sotnikov, V.T. Uvarov, and Yu.F. Filippov. Auto-oscillatory system based on dielectric resonator with whispering-gallery modes // *Technical Physics Letters*. 2012, v. 38, iss. 1, p. 85-88.
4. K.V. Galaydych, Yu.F. Lonin, A.G. Ponomarev, Yu.V. Prokopenko, and G.V. Sotnikov. Mathematical model of an excitation by electron beam of "whispering gallery" modes in cylindrical dielectric resonator // *Problems of Atomic Science and Technology. Series "Plasma Physics"*. 2010, №6, p. 123-125.
5. K.V. Galaydych, Yu.F. Lonin, A.G. Ponomarev, Yu.V. Prokopenko, and G.V. Sotnikov. Nonlinear analysis of mm waves excitation by high-current REB in dielectric resonator // *Problems of Atomic Science and Technology. Series "Plasma Physics"*. 2012, №6, p. 158-160.
6. V.A. Avgustinovich, S.N. Artemenko, A.I. Mashchenko, A.S. Shlapakovskii, and Yu.G. Yushkov. Demonstrating gain in a dielectric Cherenkov maser with a rod slow-wave system // *Technical Physics Letters*. 2010, v. 36, iss. 3, p. 244-247.
7. Yu.O. Averkov, Yu.V. Prokopenko, and V.M. Yakovenko. The instability of hollow electron beam interacting with plasma-like medium // *Telecommunications and radio engineering*. 2016, v. 75, iss. 16, p. 1467-1482.
8. Yu.O. Averkov, Yu.V. Prokopenko, and V.M. Yakovenko. Interaction between a tubular beam of charged particles and a dispersive metamaterial of cylindrical configuration // *Physical Review E*. 2017, v. 96, iss. 1, 013205.
9. A.Ya. Kirichenko, Yu.V. Prokopenko, Yu.F. Filippov, and N.T. Cherpak. *Quasi-optical solid-state resonators*. Kiev: "Naukova dumka", 2008, 286 p. (in Ukrainian).
10. V.E. Pahomov. To the Vavilov-Cerenkov radiation theory in anisotropic media with boundaries // *Proceedings of the Lebedev physics institute.* 1961, v. 16, p. 94-139.
11. V.P. Silin. Electromagnetic waves in artificial periodic structures // *Uspephi fizicheskikh nauk.* 2006, v. 175, iss. 5, p. 562-565. [*Physics-Uspekhi.* 2006, v. 49, iss. 5, p. 542-545] (in Russian).
12. N.L. Dmitruk, V.G. Litovchenko, V.L. Strizhevskiy. *Surface polaritons in semiconductors and dielectrics.* Kiev: "Naukova dumka", 1989, 376 p. (in Ukrainian).
13. A. Kolomenskiy. Cherenkov radiation and polarization losses in a uniaxial crystal // *Proceedings of the USSR academy of sciences.* 1952, v. 86, iss. 6, p. 1097-1099.
14. Yu. O. Averkov, Yu. V. Prokopenko, V. M. Yakovenko. Instability of a tubular electron beam moving over a dielectric cylinder // *Technical Physics.* 2017, v. 62, iss. 10, p. 1578-1584.
15. L. A. Vaynshteyn, V. A. Solntsev. *Lectures on ultrahigh-frequency electronics*. Moscow: "Sovetskoe Radio", 1973, 400 p. (in Russian).
16. M. V. Kuzelev, A. A. Rukhadze, and P. S. Strelkov. *Plasma relativistic microwave electronics*. Moscow: Publishing House of the N. E. Bauman Moscow State Technical University, 2002, 544 p.
17. R. S. Brazis. Active and nonlinear interactions under the excitation of plasma-type polaritons in semiconductors // *Lithuanian physical collection*. 1981, v. 21, iss. 4 p. 73-117.
18. N. N. Beletskiy, V. M. Svetlichniy, D. D. Khalameyda, V. M. Yakovenko. *Electromagnetic phenomena of microwave in inhomogeneous semiconductor structures*. Kiev: "Naukova dumka", 1991, 215 p. (in Ukrainian).
19. A. I. Akhiezer, I. A. Akhiezer, R. V. Polovin, A. G. Sitenko, and K. N. Stepanov. *Plasma electrodynamics. V.1. Linear Theory*. Oxford-New-York: "Pergamon press", 1975, 428 p.
20. A. P. Vinogradov, A. V. Dorofeenko, A. M. Merzlikin, A. A. Lisyansky. Surface states in photonic crystals // *Uspephi fizicheskikh nauk.* 2010, v. 180, iss. 3, p. 249-263. [*Physics-Uspekhi.* 2010, v. 53, iss. 3, p. 243-257] (in Russian).
21. A. Barannik., N. Cherpak, A. Kirichenko., Yu. Prokopenko, S. Vitusevich, and V. Yakovenko. Whispering gallery mode resonators in microwave physics and technologies // *Int. Journal of microwave and wireless technologies*. 2017, v. 9, iss. 4, p. 781-796.
22. P.A. Sturrock. Non-linear effects in electron plasmas // *Proceedings of the royal society A.* 1957, v. 242, iss. 1230, p. 277-299.
23. Yu.V. Bobilev, M.V. Kuzelev. *Nonlinear phenomena in electromagnetic interactions of electron beams with plasma*. Moscow: "PhysMathLitt", 2009, 456 p. (in Russian).
24. R. Kompfner. *The invention of the traveling-wave tube.* San Francisco: "San Francisco press", 1964, 30 p.
25. D.I. Trubetskov and A.E. Hramov. *Lectures on ultrahigh-frequency electronics for physicists. V.1*. Moscow: "PhysMathLitt", 2003, 496 p. (in Russian).

Article received 16.05.2018

ВЗАИМОДЕЙСТВИЕ ТРУБЧАТОГО ПУЧКА ЗАРЯЖЕННЫХ ЧАСТИЦ С АНИЗОТРОПНЫМ ДИСПЕРГИРУЮЩИМ ТВЕРДОТЕЛЬНЫМ ЦИЛИНДРОМ

Ю.О. Аверков, Ю.В. Прокопенко, В.М. Яковенко

Изучено взаимодействие нерелятивистского трубчатого потока заряженных частиц с немагнитной анизотропной диспергирующей средой цилиндрической конфигурации. Обнаружена абсолютная неустойчивость объёмно-поверхностных волн, обусловленная особенностями свойств анизотропного цилиндра. Резонансный характер частотных зависимостей диэлектрической проницаемости цилиндра приводит к появлению участков дисперсионных кривых собственных объёмно-поверхностных волн *E*-типа с отрицательной групповой скоростью. Показано существование в цилиндре собственных поверхностных волн *E*-типа и псевдоповерхностных волн *E*- и *H*-типов.

ВЗАЄМОДІЯ ТРУБЧАСТОГО ПУЧКА ЗАРЯДЖЕНИХ ЧАСТИНОК З АНІЗОТРОПНИМ ДИСПЕРГУЮЧИМ ТВЕРДОТІЛЬНИМ ЦИЛІНДРОМ

Ю.О. Аверков, Ю.В. Прокопенко, В.М. Яковенко

Вивчено взаємодію нерелятивістського трубчастого потоку заряджених частинок з немагнітним анізотропним диспергуючим середовищем циліндричної конфігурації. Виявлена абсолютна нестійкість об'ємно-поверхневих хвиль, що обумовлена особливостями властивостей анізотропного циліндра. Резонансний характер частотних залежностей діелектричної проникності циліндра призводить до появи ділянок дисперсійних кривих власних об'ємно-поверхневих хвиль *E*-типу з негативною груповою швидкістю. Показано існування в циліндрі власних поверхневих хвиль *E*-типу і псевдоповерхневих хвиль *E*- та *H*-типів.